# Extreme Dispersion and Gravitational Modulation: Advancing Tests of the Aharonov–Bohm Effect

Michael T. Hatzon, Graeme R. Flower, Maxim Goryachev, Jeremy F. Bourhill, and Michael E. Tobar

Abstract - The Aharonov-Bohm (AB) effect underscores the fundamental role of electromagnetic and gravitational potentials in quantum mechanics, even in regions where classical fields vanish. In this article, we summarize and expand on our recent work on the AB effect. We explore the gravitational AB effect as a generalization of gravitational redshift, considering a quantum system in orbit around a massive body. In this scenario, time-dependent gravitational potentials give rise to sidebands in the energy spectrum, which could be detected using precision atomic clocks aboard satellites. In parallel, we extend recent investigations of the electric-scalar AB effect. By using a balanced interferometric excitation scheme in a microwave cavity, on resonance, we achieve 25 dB suppression of the electromagnetic field- while enhancing the time-varying scalar electric potential. This offers a promising platform to directly probe the electricscalar AB effect under conditions of a null electric field and a finite scalar potential. Also, it enables the realization of a resonant system exhibiting extreme dispersion. These complementary approaches provide new experimental pathways to test fundamental quantum effects in electromagnetic and gravitational potentials.

## 1. Introduction

The Aharonov–Bohm (AB) effect is a cornerstone of quantum mechanics, demonstrating that potentials can directly influence quantum systems despite the lack of classical fields [1–3]. Initially proposed in the context of electromagnetism, the AB effect shows that a charged particle can acquire a phase shift (or Berry phase [4]) when passing through a region of nonzero magnetic vector, or electric-scalar potential, even when the associated electric and magnetic fields are absent. This phase shift theoretically leads to observable interference effects [3, 5], highlighting the fundamental role of potentials in quantum theory. Although there is experimental evidence of interactions with the magnetic vector potential [6–8], and combined magnetic vector and electric-scalar potential measurements

Manuscript received 6 March 2025.

Michael T. Hatzon, Graeme R. Flower, Maxim Goryachev, Jeremy F. Bourhill, and Michael E. Tobar are with The University of Western Australia, 35 Stirling Highway, Perth, 6009 Western Australia, Australia; e-mail: michael.hatzon@research.uwa.edu.au, graeme.flower@uwa.edu.au, maxim.goryachev@uwa.edu.au, jeremy.bourhill@uwa.edu.au, michael.tobar@uwa.edu.au.

[9], there are no experiments isolating the effect of the electric-scalar potential.

Beyond its electromagnetic origins, recent theory has extended the AB effect to the splitting of energy levels of a quantum system (i.e., the appearance of energy sidebands) [10, 11], rather than only interference effects. The gravitational AB effect arises due to the interaction between quantum systems and time-dependent gravitational potentials, predicting frequency modulations in atomic clocks in eccentric orbits. We show that this effect generalizes the gravitational redshift, showing that in addition to a constant frequency shift, atomic clocks should exhibit sidebands due to the time-varying nature of the gravitational potential. The study of these sidebands provides a novel avenue for testing general relativity and the interaction between gravity and quantum mechanics.

Similarly, the electric-scalar AB effect predicts that a quantum system enclosed within a region with a time-varying electric potential, but no electric field, should acquire energy sidebands. This effect has been challenging to experimentally observe due to the difficulty of creating a purely time-dependent scalar potential without residual electric fields. However, our experimental advancements using microwave cavity resonators have provided a platform for testing this phenomenon, achieving extreme dispersion effects through a balanced interferometric excitation scheme and allowing the necessary conditions required to scan for predicted energy level sidebands. The extreme dispersion feature results from a suppressed electric field, analogous to electromagnetically induced absorption [12–16].

This article summarizes our contributions to recent theoretical and experimental advancements in the study of the gravitational and electric-scalar AB effects. The gravitational AB effect is analyzed within the context of atomic clocks in space, while the electric-scalar AB effect is examined through controlled laboratory experiments in microwave resonators. By exploring these phenomena, we gain deeper insight into the fundamental role of potentials in quantum mechanics and implications for precision metrology and fundamental physics.

# 2. Gravitational Energy Level Splitting

The gravitational AB effect can be understood as a generalization of the gravitational redshift [1]. When a quantum system experiences a time-dependent gravitational potential, its energy levels shift, leading to the emergence of modulation sidebands in atomic transition frequencies. This effect is particularly relevant for precision

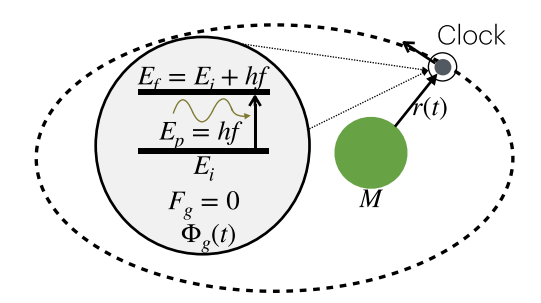


Figure 1. A clock in an elliptical orbit of distance r(t) around a massive object with mass M. The satellite in free-fall passes through a time-varying scalar potential  $\Phi_g(t)$  and experiences no gravitational force  $F_g$ . The clock has a ground state  $E_i$  and excited state  $E_f$ , separated by energy equivalent to that of absorbing a photon  $E_p = hf$ , with photon frequency f and Planck's constant h.

atomic clocks in space, where satellites in eccentric orbits experience a varying gravitational potential, but no gravitational field due to Einstein's equivalence principle.

To begin the theoretical framework, we consider an atomic clock as a two-level system undergoing continuous Rabi oscillations between its ground and excited states, seen in Figure 1. The gravitational potential modifies the energy levels of the system, leading to a phase accumulation described by the gravitational AB phase

$$\varphi_g(t) = \frac{m_e}{\hbar} \int_0^t \Phi_g(t) dt \tag{1}$$

with  $\hbar$  the reduced Planck's constant,  $m_e$  the mass of the ground state electron, and  $\Phi_g(t)$  the time-varying gravitational potential at time t. In the presence of a time-varying gravitational potential, we obtain the energy levels

$$E_i(t) = E_{i0} + m_e \Phi_e(t) \tag{2}$$

and

$$E_f(t) = E_{f0} + m_e^* \Phi_g(t)$$
 (3)

where  $E_{i0}$  and  $E_{f0}$  are the ground and excited energy levels in a zero gravitational potential. Notably,  $m_e^* = m_e + \frac{hf_p}{c^2}$ ; the effective mass of the electron has increased according to the mass–energy relation  $E = mc^2$ , and we have added the kinetic mass of the photon  $hf_p/c^2$  with  $f_p$  the photon frequency. By formulating the Hamiltonian and following the derivation procedure in [1], we acquire the solution to the two-level system wave function

$$\Psi_{f}(\mathbf{r},t) = \Psi_{f}(\mathbf{r}) \sum_{n=-\infty}^{\infty} (-1)^{n} J_{n}(\alpha)$$

$$\times \exp\left(-\frac{i(\Delta E_{0}(1 + \frac{2GM}{(r_{a} + r_{p})c^{2}}) - n\hbar\Omega)t}{\hbar}\right)$$
(4)

for orbital angular frequency  $\Omega$ , and internal coordinates  $\mathbf{r}$ . Here, G is Newton's gravitational constant, c is the

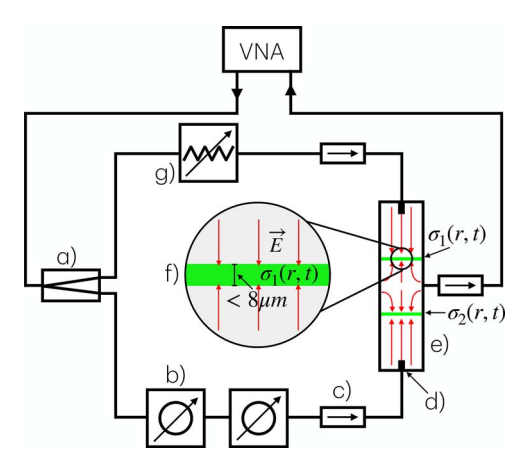


Figure 2. The experimental configuration used to achieve a suppressed electric field, while maintaining a time-varying scalar electric potential. (a) Power splitter, (b) variable attenuator, (c) isolator, (d) resonator tuning rod, (e) triple microwave cavity resonator separated by copper foils, (f) copper foil with thickness  $<8~\mu m$ , and (g) variable attenuator. The schematic electric field distribution at (e), shown by the green arrows, highlights the slice along the resonator where the fields are suppressed.

speed of light, and  $\Delta E_0 = E_{f0} - E_{i0} = h f_{p0}$ , with  $f_{p0}$  the photon and clock frequency in a zero gravitational potential. Bessel functions of the *n*th kind  $J_n(\alpha)$  are produced from a Jacobi–Anger expansion at  $\alpha$ , the modulation parameter

$$\alpha = \left(\frac{r_a - r_p}{(r_a + r_p)^2}\right) \left(\frac{2GM}{c^2}\right) \left(\frac{2\pi f_{p0}}{\Omega}\right) \tag{5}$$

with apogee and perigee radii  $r_a$  and  $r_p$ , respectively. Finally, we can extract the energy levels of this wave function

$$\Delta E(n) = \Delta E_0 \left( 1 + \frac{2GM}{(r_a + r_p)c^2} \right) \pm n\hbar\Omega = \Delta E \pm n\hbar\Omega$$
(6)

retrieving the gravitational redshift here  $\Delta E \equiv \Delta E_0(1 + \frac{SQ}{1/2 + \frac{SQ}$ 

### 3. Extreme Dispersion Resonator

Our recent experimental work has focused on probing the electric-scalar AB effect using a highly controlled microwave cavity resonator [2]. This setup, shown in Figure 2, uses a balanced interferometric excitation scheme and a unique microwave cavity resonator to suppress the resonant electromagnetic field, while maintaining a time-varying scalar electric potential, a crucial condition for testing the electric-scalar AB effect.

The microwave cavity is a triple resonator system separated by two thin copper foils, allowing  $TM_{010}$  modes from the upper and lower resonator to deposit

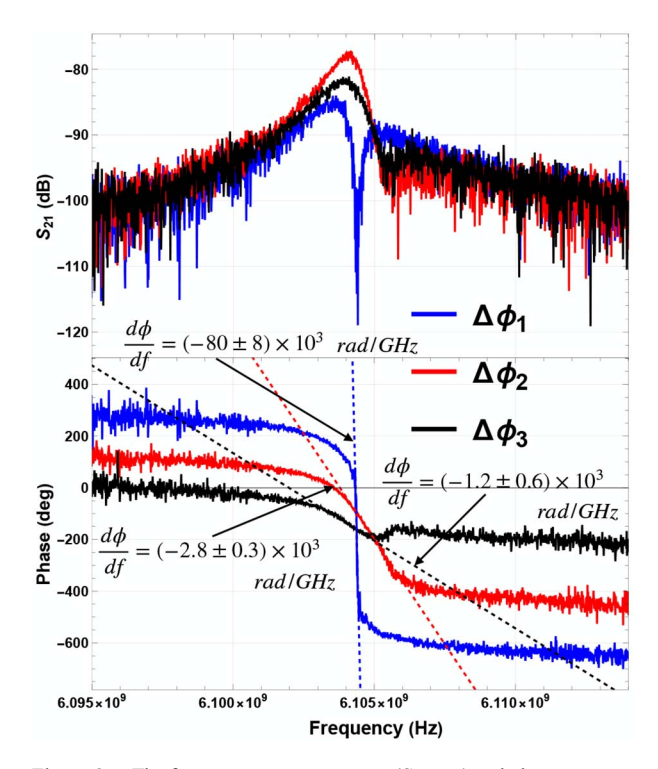


Figure 3. The frequency response spectra  $(S_{21}, \text{top})$  and phase response (degree, bottom) of the circuit at three different relative phase differences,  $\Delta\phi_1=0,\,\phi_2=\pi$ , and an intermediate  $0<\phi_3<\pi$ . The blue spectra correspond to the case of electric field cancellation at the resonant frequency, suggesting  $\Delta\phi_1\approx 0$ , with a phase response an order of magnitude larger than for other phases.

an effective charge onto the foil, allowing it to excite the central microwave resonator. Using Gauss's law and the standard electric field structure of the  $TM_{010}$  mode, the charge density phasors on the top and bottom foil, respectively, within the central resonator take the form

$$\widetilde{\sigma}_{1,2}(r,t) = \sigma_{01,02} J_0(\chi_{0,1} r/R) e^{i\omega t + \phi_{1,2}}$$
 (7)

with  $\chi_{0.1}$  the first root of the first-kind Bessel function, with a value of 2.405, and r is the radial coordinate. A complete derivation can be seen in [2]. The phase term  $e^{i\omega t + \phi_{1,2}}$  at frequency and time  $\omega$  and t, highlights how we obtain phase control  $\phi_{1,2}$  of each charge density phasor due to the phase shifters shown in Figure 2. Also, the charge density magnitudes  $\sigma_{01,02}$  are matched with the capabilities of the introduced variable attenuator. Matching the phase and amplitude of the charge density distribution on the central resonator foils precisely is the condition required to cancel the electric and magnetic field within the central resonator component. The fields are perfectly suppressed along a slice through the resonator, with an effective suppression in the volume element nearby this slice. The effect of changing the relative phase  $\Delta \phi = \phi_2 - \phi_1$  between the two resonators is shown in Figure 3.

The asymmetry in Figure 3 is due to nonideal balance conditions such as ensuring all three resonators precisely have the same resonant frequency, power entering the resonators (that powers the TM<sub>010</sub> modes and hence charge buildup on both foils), and  $\pi$  the phase difference between the interferometer arms. By optimizing these parameters into antiresonance on the transfer function, a phase response an order of magnitude larger than the relative resonance condition, as well as around 25 dB of field suppression can be achieved. We have achieved an extreme dispersion regime analogous to electromagnetically induced absorption, where sharp absorption features emerge due to destructive interference between excitation pathways. The result is a system in which the energy shifts of quantum states can be studied in the presence of a pure potential, without classical field contributions when excited at this suppressed frequency. This experimental framework provides a novel pathway for investigating fundamental quantum mechanical effects and could pave the way for future precision measurements that distinguish potential-induced phase shifts from conventional field interactions.

# 4. Conclusion

The exploration of both the gravitational and electric-scalar AB effects has broad implications for quantum field theory, precision metrology, and fundamental physics. The latest theoretical understanding of the gravitational AB effect offers a new avenue for testing general relativity in the quantum regime, potentially informing the development of quantum gravity theories. The electric-scalar AB effect, if experimentally confirmed, would provide further evidence of the physical significance of potentials beyond traditional classical interpretations.

Future work may focus on refining the experimental setup to achieve even greater suppression of unwanted fields while maintaining strong potentials, as well as placing a quantum system such as a nitrogen-vacancy diamond center in this region to actually scan for the predicted energy level shifts as a test of the electric-scalar AB effect. In addition, precise space-based experiments using optical atomic clocks could scan with high sensitivity the gravitational AB effect. With advancements in both theoretical modeling and experimental techniques, we may be on the brink of understanding and detecting of these elusive quantum phenomena.

For now, the AB effect remains one of the most intriguing demonstrations of the fundamental role of potentials in quantum mechanics. Our recent theoretical work has extended the AB effect to gravitational systems, predicting measurable sidebands in orbiting atomic clocks due to time-dependent gravitational potentials. Our experimental efforts have also made significant strides in probing the electric-scalar AB effect using microwave cavity resonators. The electric field suppression resonator with increased phase response is not only useful in the field of precision metrology but also provides the conditions required to test the illusive electric-scalar AB effect. Together, these advances contribute to our understanding of quantum potentials and the impact on physical systems, opening new directions

for both fundamental research and practical applications in precision measurement technologies.

# 5. References

- M. E. Tobar, M. T. Hatzon, G. R. Flower, and M. Goryachev, "Scalar Gravitational Aharonov–Bohm Effect: Generalization of the Gravitational Redshift," *Applied Physics Letters*, 125, 9, August 2024, p. 094002.
- M. T. Hatzon, G. R. Flower, M. Goryachev, J. F. Bourhill, and M. E. Tobar, "Sharp Electromagnetically Induced Absorption via Balanced Interferometric Excitation in a Microwave Resonator," *Physical Review Applied*, 23, 2, February 2025, p. 024058.
- Y. Aharonov and D. Bohm, "Significance of Electromagnetic Potentials in the Quantum Theory," *Physical Review*, 115, 3, August 1959, p. 485.
- M. V. Berry, "Quantal Phase Factors Accompanying Adiabatic Changes," *Proceedings of the Royal Society of London* A: Mathematical and Physical Sciences, 392, 1802, March 1984, pp. 45-57.
- Y. Aharonov and D. Bohm, "Further Considerations on Electromagnetic Potentials in the Quantum Theory," *Physical Review*, 123, 4, August 1961, p. 1511.
- C. Phatak, A. K. Petford-Long, and M. De Graef, "Three-Dimensional Study of the Vector Potential of Magnetic Structures," *Physical Review Letters*, 104, 25, June 2010, p. 253901.
- 7. R. Chambers, "Shift of an Electron Interference Pattern by Enclosed Magnetic Flux," *Physical Review Letters*, **5**, 1, July 1960, p. 3.
- A. Tonomura, N. Osakabe, T. Matsuda, T. Kawasaki, J. Endo, et al., "Evidence for Aharonov-Bohm Effect With Magnetic

- Field Completely Shielded from Electron Wave," *Physical Review Letters*, **56**, 8, February 1986, p. 792.
- A. Van Oudenaarden, M. H. Devoret, Y. V. Nazarov, and J. Mooij, "Magneto-Electric Aharonov-Bohm Effect in Metal Rings," *Nature*, 391, 6669, February 1998, pp. 768-770.
- R. Chiao, N. Inan, M. Scheibner, J. Sharping, D. Singleton, et al., "Gravitational Aharonov-Bohm Effect," *Physical Review D*, 109, 6, March 2024, p. 064073.
- R. Chiao, H. Hart, M. Scheibner, J. Sharping, N. Inan, et al., "Energy-Level Shift of Quantum Systems via the Scalar Electric Aharonov-Bohm Effect," *Physical Review* A, 107, 4, April 2023, p. 042209.
- 12. A. Lezama, S. Barreiro, and A. Akulshin, "Electromagnetically Induced Absorption," *Physical Review A*, **59**, 6, June 1999, p. 4732.
- D. Brazhnikov, S. Ignatovich, V. Vishnyakov, R. Boudot, and M. Skvortsov, "Electromagnetically Induced Absorption Scheme for Vapor-Cell Atomic Clock," *Optics Express*, 27, 25, December 2019, pp. 36034-36045.
- A. B. Yelikar and R. Pant, "Analogue of Electromagnetically Induced Absorption in the Microwave Domain Using Stimulated Brillouin Scattering," *Communications Physics*, 3, 1, June 2020, p. 109.
- H. Dong, C. Gao, L. Zeng, D. Zhang, and H. Zhang, "Investigating on the Electromagnetically Induced Absorption Metamaterial in the Terahertz Region Realized by the Multilayer Structure," *Physica B: Condensed Matter*, 639, August 2022, p. 413936.
- X. Zhang, N. Xu, K. Qu, Z. Tian, R. Singh, et al., "Electromagnetically Induced Absorption in a Three-Resonator Metasurface System," *Scientific Reports*, 5, 1, May 2015, p. 10737.